Structural Health Monitoring of Ribbon Reinforced Composite Laminate using Piezoelectric Sensory Layer

ARTICLE *in* INTERNATIONAL JOURNAL OF COMADEM · JANUARY 2008

3 AUTHORS, INCLUDING:

Bishakh Bhattacharya
Indian Institute of Technology Kanpur
62 PUBLICATIONS **150** CITATIONS

Structural Health monitoring of Ribbon Reinforced Composite Laminate using Piezoelectric Sensory Layer

Arvind Kumar Jaiswal, Anand Kumar and Bishakh Bhattacharya*

Department of Mechanical Engineering, IIT-Kanpur, Kanpur 208016

Abstract:

The ribbon reinforced composites are widely used in prosthetics – for example, in the field of orthodontics where canine to canine retention is carried out with the help of resin composite retainers reinforced with Polyethylene/Kevlar ribbons. These structures typically work like a bridge between the canines. They are subjected to central loading as well as support yielding due to unequal movement of the of the end supports. However, due to the high strain in the laminate, the chances of delamination and laminate failures are quite high in such structures. The present work has proposed a high precision piezoelectric finite element which can be used with a piezoelectric sensory network to identify a damage signal and help in early replacement of the bridge. In order to identify the damage the voltage profile and mechanical impedance are obtained for healthy and damaged laminate which can be used as a data-base for fault detection.

* For Correspondence: Dr. Bishakh Bhattacharya, Department of Mechanical Engineering, IIT-Kanpur, Kanpur 208016, India
e-mail: bishakh@iitk.ac.in, Tel: +91-512-259-7824 (O) Fax: +91-512-259-7408

1. Introduction

The structural advantages of laminated composites are often compromised due to the presence of hidden defects. Damages such as delamination, ply failure or crack in the matrix may lead to the severe reduction in the load bearing capacity of a composite. Ribbon reinforced composite laminate, for example, are widely used in the field of orthodontics where canine-to-canine retention is carried out with the help of resin composite retainers reinforced with polyethylene/ Kevlar ribbons. These structures typically work like a bridge between the canines. They are subjected to central loading as well as support yielding due to unequal displacement of the two end supports. This farther generates large strain in the laminate and the chances of delamination and laminate failures are quite high in such composite. Therefore, it is important to develop a technique for monitoring the severity, type and location of damage in such composites. Experimental damage monitoring mainly involves non-destructive sensing of the damage in the structure such as using ultrasonic, magnetic field or X-ray based scanning etc. Many of these methods of identification involve experimental techniques which are quite expensive and also difficult for applications related to prosthetics.

Chung [1] has developed an electrical resistance method for structural health monitoring of composite materials. It is limited to composite materials which are electrically conductive such as composites with carbon fibers. Pandey et al [2] have developed a damage identification technique based on curvature of mode shapes. They have shown that the absolute difference in the curvature of mode shapes between the

healthy and the damaged ply may be used as a parameter for predicting the damage and the damage location. This concept has been applied to a vibrating flat plate with the assumption that the modulus of elasticity in the damaged area becomes equal to zero. Liu et al [3] have shown that embedded piezoelectric sensors can act as wave transmitters as well as sensors. The evaluation of the structural status can thus be monitored using information carried by waves propagating in the structure and interacting with any internal damage. Coverley and Staszewski [4] have shown that using a classical sensor triangulation scheme and a Genetic Algorithm procedure the impact location can be accurately identified. This procedure substantially alleviates the complexity in learning and matching and thus becomes computationally efficient.

The present work has proposed knowledge based piezoelectric sensory system which can identify the damage signal and help in early replacement of the bridge. In order to identify the damage a voltage profile and mechanical impedance is developed both for healthy composite and damaged ply. Finite element analysis using high precision element are carried out in this paper to identify the damage signals accurately.

Cowper [7] developed a high precision bending element of arbitrary triangular shape and applied to the solution of several static and dynamic passive plate problems. Lindberg et al [8] developed a high precision cylindrical shell finite element. Jeyachandrabose and Kirkhope [9] presented an efficient formulation for eighteen degree of freedom high precision bending element also they & B. Bhattacharya [10] developed an efficient formulation of the stiffness matrix for a high precision triangular laminated anisotropic finite element. The formulation is based on classical lamination theory. This consistent

methodology is followed here. The results of dynamic analysis are expected to help in efficient damage diagnosis for these kinds of structures.

2. Piezoelectric Voltage Sensing in Laminated Composite

This section briefly describes the finite element formulation of Smart Laminated Composite Plate and the voltage sensed by embedded Piezo-electric layers during vibration.

2.1 Constitutive Relationship of Laminated Composite

The composite plate is modelled in this paper following CLPT (Classical Laminated Plate Theory). The derivations related to macro mechanics of composites are common text book material [] – however they are briefly discussed here for the sake of completeness. Considering the deformation of a laminate in x-z plane (as shown in Figure 1) and assuming that normal to the mid plane remain straight and normal after deformation the strain-displacement relations for a point at a distance z from the middle surface of the laminate are given by equations (1-4):

$$\varepsilon_x = \frac{\partial u}{\partial x} - z\frac{\partial^2 w}{\partial x^2} \tag{1}$$

$$\varepsilon_y = \frac{\partial v}{\partial x} - z\frac{\partial^2 w}{\partial y^2} \tag{2}$$

$$\gamma_{xy} = \frac{\partial u}{\partial y} + \frac{\partial v}{\partial x} - 2z\frac{\partial^2 w}{\partial x \partial y} \tag{3}$$

or $$\begin{Bmatrix} \varepsilon_x \\ \varepsilon_y \\ \gamma_{xy} \end{Bmatrix} = \begin{Bmatrix} \varepsilon_x^0 \\ \varepsilon_y^0 \\ \gamma_{xy}^0 \end{Bmatrix} + z\begin{Bmatrix} k_x \\ k_y \\ k_{xy} \end{Bmatrix} \tag{4}$$

Where $\{\varepsilon^o\} = \begin{Bmatrix} u_{,x} \\ u_{,y} \\ u_{,y} + v_{,x} \end{Bmatrix}$ is the mid plane strain vector, $\{\kappa\} = \begin{Bmatrix} -w_{,xx} \\ -w_{,yy} \\ -2w_{,xy} \end{Bmatrix}$ is the curvature vector; and u, *v* and *w* are the mid plane displacements.

Following the standard notations of laminated composite theory, the constitutive relationship for any *k*-th layer of laminate with respect to the principal material axis is given by:

$$\begin{Bmatrix} \sigma_1 \\ \sigma_2 \\ \sigma_{12} \end{Bmatrix}_k = \begin{bmatrix} Q_{11} & Q_{12} & 0 \\ Q_{12} & Q_{22} & 0 \\ 0 & 0 & Q_{66} \end{bmatrix}_k \begin{Bmatrix} \varepsilon_1 \\ \varepsilon_2 \\ \varepsilon_{12} \end{Bmatrix}_k \tag{5}$$

where, Q is known as the reduced stiffness matrix; the elements of Q matrix are functions of the elastic constants and Poisson's ratio of the layer

The constitutive relation may be farther transformed from the principal axes of each lamina to the global coordinate system *x*-*y*-*z* by:

$$\begin{Bmatrix} \sigma_x \\ \sigma_y \\ \sigma_{xy} \end{Bmatrix} = \begin{bmatrix} \overline{Q}_{11} & \overline{Q}_{12} & \overline{Q}_{16} \\ & \overline{Q}_{22} & \overline{Q}_{26} \\ sym & & \overline{Q}_{66} \end{bmatrix} \begin{Bmatrix} \varepsilon_x \\ \varepsilon_y \\ \varepsilon_{xy} \end{Bmatrix} \tag{6}$$

Where the transformed matrix $\bar{Q}$ is given by:

$$\bar{Q} = [T]_{\sigma}^{-1} Q [T]_{\varepsilon}$$

$$[T]_{\sigma} = \begin{bmatrix} m^2 & n^2 & 2mn \\ n^2 & m^2 & -2mn \\ -mn & mn & m^2 - n^2 \end{bmatrix} \quad [T]_{\varepsilon} = \begin{bmatrix} m^2 & n^2 & mn \\ n^2 & m^2 & -mn \\ -2mn & 2mn & m^2 - n^2 \end{bmatrix} \tag{7}$$

In which $m = \mathrm{Cos}\,\theta$ and $n = \mathrm{Sin}\,\theta$; θ being the fibre angle which is the angle between the global axes *x -y-z* and the principal axis of each lamina 1-2-3.

The resultant forces and moments per unit length in a cross-section may be obtained by integrating the corresponding stresses through the laminate of thickness h and are given by the equations (8-11).

$$\begin{Bmatrix} N_x \\ N_y \\ N_{xy} \end{Bmatrix} = \sum_{k=1}^{n} \int_{h_{k-1}}^{h_k} \begin{Bmatrix} \sigma_x \\ \sigma_y \\ \sigma_{xy} \end{Bmatrix} dz \tag{8}$$

and

$$\begin{Bmatrix} M_x \\ M_y \\ M_{xy} \end{Bmatrix} = \sum_{k=1}^{n} \int_{h_{k-1}}^{h_k} \begin{Bmatrix} \sigma_x \\ \sigma_y \\ \sigma_{xy} \end{Bmatrix} z dz \tag{9}$$

Where *N* are the membrane forces, *M* are the bending moments, n = total no. of layers. Hence, the constitutive relationship for the complete laminate are given by,

$$\begin{Bmatrix} N \\ M \end{Bmatrix} = \begin{bmatrix} A & B \\ B & D \end{bmatrix} \begin{Bmatrix} \varepsilon_0 \\ \kappa \end{Bmatrix} \tag{10}$$

[A], [B]and [D] are the effective membrane, bending membrane coupling stiffness and bending stiffness matrix of the laminate defined as,

$$\left(A_{ij}, B_{ij}, D_{ij}\right) = \sum_{k=1}^{n} \int_{h_k}^{h^{k+1}} \left(\overline{Q}_{ij}\right)_k \left(1, z, z^2\right) dz \tag{11}$$

2.2 Development of Element Stiffness Matrix:

The finite element used here is based on a 38 DOF freedom triangular plate bending element developed by Jeychandrabose and Kirkhope [] and later extended by Bhattacharya et al [] for dynamic analysis.

The element properties are derived using the area coordinate system ξ, η and ς. These coordinates are related to the Cartesian coordinate as:

$$\xi = \frac{a_1 + b_1 x + c_1 y}{2\Delta} \tag{12}$$

$$\eta = \frac{a_2 + b_2 x + c_2 y}{2\Delta} \tag{13}$$

$$\varsigma = 1 - \xi - \eta \tag{14}$$

Where,

$$\Delta = \frac{1}{2}\begin{vmatrix} 1 & x_1 & y_1 \\ 1 & x_2 & y_2 \\ 1 & x_3 & y_3 \end{vmatrix}$$

and,

$a_i = x_j y_k - x_k y_j$,

$b_i = y_j - y_k$,

$c_i = x_k - x_j$.

Here i, j, k = 1, 2, 3 in cyclic order, (x_n, y_n) n= 1, 2, 3 are the global coordinates of the three vertices of the triangle in Cartesian system and Δ denotes and area of the triangular element.

In each element, three field displacements u, v (in plane components) and w (transverse component) along x, y and xz directions are considered. Nodal DOF chosen are grouped into three vectors as,

$$\{\delta\}^T = \left\{\{U\}^T, \{V\}^T, \{W\}^T\right\} \tag{15}$$

Where,

$$\{U\}^T = \{u_1, u_{x1}, u_{y1}, u_2, ..., u_{y3}, u_c\}_{10\times 1}$$

$$\{V\}^T = \{v_1, v_{x1}, v_{y1}, v_2, ..., v_{y3}, v_c\}_{10\times 1}$$

$$\{W\}^T = \{w_1, w_{x1}, w_{y1}, w_{xx1}, w_{xy1}, w_{yy1}, w_2, ..., w_{yy3},\}_{18\times 1} \tag{16}$$

u_x, w_x, etc. are the first order derivatives with respect to at the node i (i = 1,2,3). Similarly, w_{xx}i, etc. are the second order derivatives; u_c, v_c denote the displacements along x and y direction at the centroid of the element. The in plane displacement functions are assumed to be complete cubic polynomial such as,

$$u(\xi,\mu) = C_1 + C_2\xi + C_3\eta + C_4\xi^2 + C_5\xi\eta$$
$$+C_6\eta^2 + C_7\xi^3 + C_8\xi^2\eta + C_9\xi\eta^2 + C_{10}\eta^3$$

or, $u(\xi,\eta)=\{\Lambda_1\}^T\{C\}$ (17)

W`here $\{\Lambda_1\}^T=\{1,\xi,\eta....,\eta^3\}$ and

$\{C\}^T=\{C_1,.....,C_{10}\}$

A quintic polynomial series is adopted for the transverse displacement function:

$w(\xi,\eta)=\{\Lambda_2\}^T\{\overline{C}\}$ (18)

Where $\{\Lambda_2\}^T=\{1,\xi,\eta,.....\eta^4,\xi^5,\xi^3\eta^2,\xi^2\eta^3,\xi\eta^4,\eta^5,\}_{1\times21}$

The in plane displacement u can be written as:

$u(\xi,\eta)=[N]\{U\}$ (19)

$v(\xi,\eta)=[N]\{V\}$ (20)

Similarly transverse displacement can be written as:

$w(\xi,\eta)=[\overline{N}]\{W\}$ (21)

Where, $[\mathrm{N}]=\{\Lambda_1\}^{\mathrm{T}}[\mathrm{R}]$

and $[\overline{\mathrm{N}}]=\{\Lambda_2\}^{\mathrm{T}}[\mathrm{S}]$

Where, [R] and [S] is the transformation matrix between natural and global coordinates. Closed form expressions of these two matrices are reported in [9] and [10].

The strain energy of a thin laminated plate element is given by integral over the element.

$$U_s = \frac{1}{2}\int\int\left\{\{N\}^T\{\varepsilon^0\} + \{M\}^T\{\kappa\}\right\}dxdy \tag{22}$$

Substituting equation (15) into equation (27) we get the Strain energy as

$$U_s = \frac{1}{2}\int_A \{\varepsilon^o\}^T[A]\{\varepsilon^o\} + \{\varepsilon^o\}^T[B]\{\kappa\} + \{\varepsilon^o\}\{\kappa\}^T[B] + \{\kappa\}^T[D]\{\kappa\}\,dA \tag{23}$$

In terms of area co-ordinates,

$$\{\varepsilon^o\} = \frac{1}{2\Delta}[P]\{\alpha\} \tag{24}$$

$$\{\kappa\} = \frac{1}{2\Delta^2}[Q]\{\beta\} \tag{25}$$

Where,

$$\{\alpha\}^T = \left[u_{,\xi}, u_{,\eta}, v_{,\xi}, v_{,\eta}\right] \tag{31}$$

$$\{\beta\}^T = -\left[w_{,\xi\xi}, w_{,\eta\eta}, w_{,\xi\eta}\right] \tag{32}$$

$$[P] = \begin{bmatrix} b_1 & b_2 & 0 & 0 \\ 0 & 0 & c_1 & c_2 \\ c_1 & c_2 & b_1 & b_2 \end{bmatrix} \tag{33}$$

$$[Q]=\begin{bmatrix} b_1^2 & b_2^2 & 2b_1b_2 \\ c_1^2 & c_2^2 & 2c_1c_2 \\ 2b_1c_1 & 2b_2c_2 & 2(b_1c_2+b_2c_1) \end{bmatrix} \tag{34}$$

Substitution of equation (29) into (28), the final form of strain energy is

$$U_s=\frac{1}{2}\int_0^1\int_0^{1-\xi}\left[\{\alpha\}^T[\bar{A}]\{\alpha\}+\{\alpha\}^T[\bar{B}]\{\beta\}+\{\beta\}^T[\bar{B}]\{\alpha\}+\{\beta\}^T[\bar{D}]\{\beta\}\right]d\xi d\eta \tag{35}$$

where

$$[\bar{A}]=\frac{1}{2\Delta}[P]^T[A][P]$$

$$[\bar{B}]=\frac{1}{(2\Delta)^2}[P]^T[B][Q]$$

$$[\bar{D}]=\frac{1}{(2\Delta)^3}[Q]^T[D][Q]$$

The strain energy in form of element stiffness matrix can also be written as:

$$2U=\begin{Bmatrix} \delta_u^T \\ \delta_v^T \\ \delta_w^T \end{Bmatrix}[K]\begin{Bmatrix} \delta_u \\ \delta_v \\ \delta_w \end{Bmatrix} \tag{36}$$

Therefore, the element stiffness matrix [K] is given by

$$[K]=\begin{bmatrix} X_{11} & X_{12} & X_{13} \\ & X_{22} & X_{23} \\ \text{sym} & & X_{33} \end{bmatrix} \tag{37}$$

where,

$$X_{11}=[R]^T[F_1][R]$$

$$X_{12}=[R]^T[F_2][R]$$

$$X_{13}=[R]^T[G_1][S]$$

$$X_{22}=[R]^T[F_3][R]$$

$$X_{23}=[R]^T[G_2][S]$$

$$X_{33}=[S]^T[H][S]$$

The Matrix $[F_1],[F_2],[G_1],[F_3],[G_2]$ and $[H]$ are defined as follows:

Mass Matrix:

The kinetic energy T, of the element is given as

$$T=\frac{1}{2}\begin{Bmatrix}\dot{u}^T\\ \dot{v}^T\\ \dot{w}^T\end{Bmatrix}^T M\begin{Bmatrix}\dot{u}\\ \dot{v}\\ \dot{w}\end{Bmatrix} \qquad (45)$$
$$=\frac{1}{2}\int_V \rho\left[\dot{u}^T\dot{u}+\dot{v}^T v+\dot{w}^T w\right]dV$$

Where, M is the mass matrix, ρ is the density of the plate and V is the volume of the element. Expressing u, v and w in terms of nodal variables U, V and W and using equation (2.22), the expression for kinetic energy may be written as:

$$T=\frac{1}{2}\int_V \rho\begin{bmatrix}\dot{U}^T N^T N\dot{U}+\dot{V}^T N^T N\dot{V}\\ +\dot{W}^T\bar{N}^T\bar{N}\dot{w}\end{bmatrix}dV \qquad (46)$$

Hence, for any composite laminate, the mass matrix can be written as:

$$M=\sum_{k=1}^{n}\Delta t_k\rho_k\iint[N_s^T N_s^T]dxdy \qquad (47)$$

Where Δt_k = thickness of the k_{th} layer, ρ_k = density per unit area of the k_{th} layer and

$$N_s=\begin{bmatrix}N & 0 & 0\\ 0 & N & 0\\ 0 & 0 & \bar{N}\end{bmatrix} \qquad (48)$$

The shape functions used to find mass matrix is same as that for field displacement. Such mass matrices are called ‘Consistent Mass Matrix’. There is another type of mass matrix

called ‘Lumped mass matrix’ where only diagonal term are present and is less populated than consistent mass matrix. Hence the consistent mass matrix is computationally more intensive but more accurate so consistent mass matrix is chosen for this problem. The expression for mass matrix on transformation to area coordinates is

$$M=\sum_{k=1}^{n} 2\Delta t_k \rho_k \Delta \int_0^1 \int_0^{1-\xi} [N_s^T N_s] d\xi d\eta \tag{49}$$

Sensor Voltage:

The linear constitutive equations of a piezoelectric layer, including the converse and direct piezoelectric effects, can be written as

$$\sigma_i = C_{ij}\varepsilon_j - e_{ki}E_k$$

$$D_l = e_{lj}\varepsilon_j + \in_{lk}^{s} E_k \tag{50}$$

where σ_i and ε_j are the stress vector and strain vector, E_k is the electric field vector, D_l is the electric displacement vector, C_{ij} is the elastic stiffness matrix, e_{ki} is the piezoelectric stress charge tensor and $\in_{lk}^{s}$ is the piezoelectric permittivity matrix. The electric field vector of the piezoelectric layer is related to the electric potential vector V by

$$E_i = -V_{,i} \tag{51}$$

It can be assumed that the electric potential functions have linear variation across the thickness of the piezoelectric and it is constant throughout the area. For the sensor layer that is poled in z direction, the electric field is absent therefore $E_3 = 0$.

The resultant stress due to mechanical deformation is

$$\begin{Bmatrix} \sigma_1 \\ \sigma_2 \\ \sigma_3 \end{Bmatrix} = [C] \begin{Bmatrix} \varepsilon_1 \\ \varepsilon_2 \\ \varepsilon_3 \end{Bmatrix} = [C][T_{m2}] \begin{Bmatrix} \varepsilon_x \\ \varepsilon_y \\ \gamma_{xy} \end{Bmatrix} \tag{52}$$

For Piezoelectric layer

$$[C] = [C_p] = \begin{bmatrix} E_p/(1-v^2) & vE_p/(1-v^2) & 0 \\ vE_p/(1-v^2) & E_p/(1-v^2) & 0 \\ 0 & 0 & E_p/2(1+v) \end{bmatrix} \tag{53}$$

E_p is the Young modulus and v is the Poisson ratio. The transformation matrix T_{m2} is

$$[T_{m2}] = \begin{bmatrix} m^2 & n^2 & mn \\ n^2 & m^2 & -mn \\ -2mn & 2mn & m^2-n^2 \end{bmatrix} \tag{54}$$

$m=\cos\theta$, $n=\sin\theta$ and θ is the skew angle.

The electric displacement on the sensor surfaces given by

$$D_3 = e_{31}\varepsilon_1 + e_{32}\varepsilon_2 = \{e_3\}^T [T_{m2}][\varepsilon_x \varepsilon_y \gamma_{xy}]^T \tag{55}$$

From Gauss law, the charge output $Q^i(t)$ of the i^{th} electroplated sensor can be expressed in terms of spatial integration of D_3 over its surface as $Q^i(t)=\sum Q_j^i(t)$ j denotes the element no. of the i^{th} sensor.

$$Q_j^i(t) = \frac{1}{2}(\iint_{A_j^+} D_3 dA + \iint_{A_j^+} D_3 dA) \tag{56}$$

If $A_j^+ = A_j^-$ then

$$Q_j^i(t) = \iint_A D_3 dA$$

D_3 in can also be written as:

$$D_3=[d_{31}d_{32}0][C][T_{m2}][B_2]\{\delta\} \tag{57}$$

Where

$$B_2 = \begin{bmatrix} \frac{\partial N}{\partial x} & 0 & -z\frac{\partial^2 \overline{N}}{\partial x^2} \\ 0 & \frac{\partial N}{\partial y} & -z\frac{\partial^2 \overline{N}}{\partial y^2} \\ \frac{\partial N}{\partial y} & \frac{\partial N}{\partial x} & -2z\frac{\partial^2 \overline{N}}{\partial x \partial y} \end{bmatrix}$$ and $\{\delta\}$ is the nodal displacement vector.

So, charge for i^{th} electroplated sensor is

$$Q^i=[B_{ds}]^i\{\delta\} \tag{58}$$

where $[B_{ds}]^i$ is the mechano-electronic matrix of the i^{th} sensor.

$[B_{ds}]^i$ in the element wise can be written as:

$$b_{ds} = \int_0^1 \int_0^{1-\xi} [d_{31} d_{32} 0][C][T_{m2}][B_2] d\xi d\eta \tag{59}$$

The output charge Q^i can be transformed into sensor voltage as:

$$\phi_s^i = G_i^c \frac{Q^i}{C_r} \tag{60}$$

Where G_i^c is the constant gain of the charge amplifier and C_r is the capacitance of the ith electroplated sensor.

3. Formulation for Mechanical Impedance:

The mechanical aspect of the structure is described by its mechanical impedance (Z_m). This includes the effect of mass stiffness, damping and boundary conditions.

The equation of motion for a general dynamical system is in the form

$$[M]\{\ddot{x}\}+[K]\{x\}=\{F(t)\} \tag{61}$$

The only assumption needed here is that M and K are positive definite. Introducing the 2n - dimensional state vector

$$q(t) = [\dot{x}^T(t) \vdots x^T(t)]^T \tag{62}$$

and the 2n-dimensional excitation vector $Q(t)=[F^T(t):0^T]^T$, equation (61) can be transformed into

$$[M^*]\{\ddot{q}\}+[K^*]\{q\}=\{Q(t)\} \tag{64}$$

Where $M^*=\begin{bmatrix} M & 0 \\ 0 & K \end{bmatrix}$ and $K^*=\begin{bmatrix} C & K \\ -K & 0 \end{bmatrix}$ are real $2n\times 2n$ matrices. But, whereas M^* is a positive definite symmetric matrix, K^* is neither positive definite nor symmetric. Using Cholesky decomposition mass matrix can be written as

$$M^* = LL^T \tag{65}$$

Then, introducing the linear transformation

$$L^Tq(t)=u(t),\quad q(t)=L^{-T}u(t) \tag{66}$$

Where $L^{-T} = (L^T) = (L^{-1})^T$, equation (63) can be reduced to

$$\dot{u}(t)=Au(t)+U(t) \tag{67}$$

in which $A=-L^{-1}K^*L^{-T}$ is a real nonsymmetric matrix and $U(t)=L^{-1}Q(t)$ is a real vector.

The solution of equation (67) can be obtained by modal analysis, which amounts to the determination of the Jordan form for A. The eigenvalue problem associated with equation (67) has the form $Au=\lambda u$. The solution consists of 2n eigenvalue λ_i and 2n eigenvectors u_i (i=1,2,.....2n) .The Jordan matrix is diagonal

$$\Lambda = diag[\lambda_i] \tag{68}$$

The eigenvectors u_i, known as right eigenvectors of A, can be arranged in the square matrix

$$U = [u_1 u_2 .....u_{2n}] \tag{69}$$

Similarly, left eigenvectors are arranged in a square matrix, as follows:

$$V = [v_1 v_2 .....v_{2n}] \tag{70}$$

The set of eigenvectors u_i is orthogonal to the set of eigenvectors v_i and eigenvectors can be normalized so as to satisfy

$$V^T U = U^T V = I \tag{71}$$

in which case Jordan matrix is simply

$$V^T AU = \Lambda \tag{72}$$

Either set of eigenvectors can be taken as a basis for L^{2n}. Hence we assume that the solution of equation has the form

$$u(t) = \sum_{i=1}^{2n} u_i z_i = Uz(t) \tag{73}$$

where z(t) is a 2n-vector with components $z_i(t)$. Substituting equation (73) into equation (67), premultiplying the result by V^T and using equations (71-72), we obtain

$$\dot{z}(t) = \Lambda z(t) + Z(t) \tag{74}$$

in which

$$Z(t) = V^T U(t) \tag{75}$$

From equation (64), the actual response is

$$q(t) = L^{-T} \sum_{i=1}^{2n} u_i z_i \tag{76}$$

The homogeneous solution of equation (65) is

$$u(t) = e^{At} u(0) \tag{77}$$

The total solution of equation (65) is

$$u(t) = e^{At}u(0) + \int_0^t e^{A(t-\tau)}U(\tau)d\tau \tag{78}$$

The actual response is

$$q(t)=L^{-T}U(e^{\Lambda t}V^{T}L^{T}q(0)+e^{\Lambda(t-\tau)}V^{T}L^{-1}Q(t)) \tag{79}$$

The velocity $\dot{x}$ can be obtained from the equation (62). The mechanical impedance of the system is

$$Z(t)=\frac{F(t)}{\dot{x}(t)} \tag{80}$$

4. Application on simple problem:

In this section convergence of voltage is studied for a simple problem

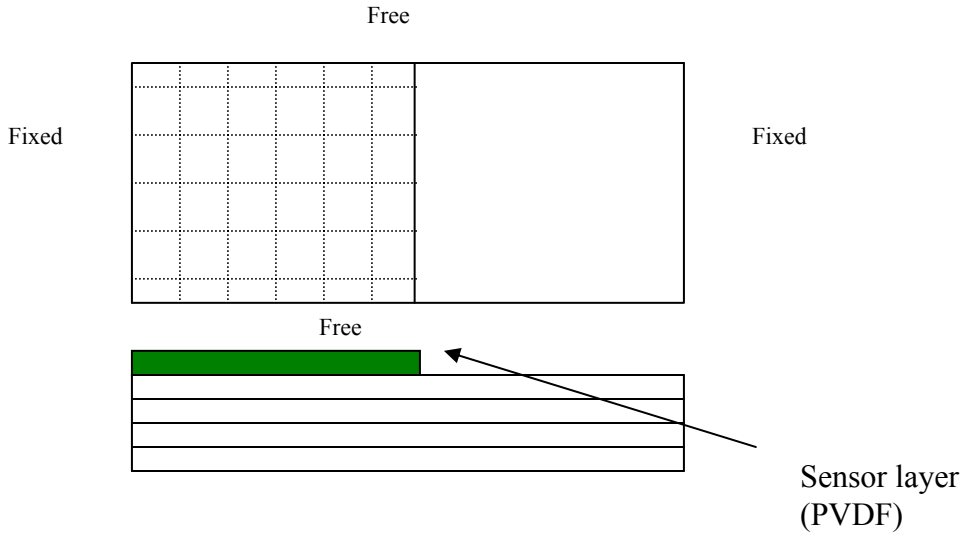

Figure1. Layout of composite plate with sensor

Laminate Detail:

Fiber: Glass Fiber,

Matrix Material: Epoxy Resin,

Mechanical Properties:

Elastic modulus of laminate

E_x = 28.45 GPa,

E_y = 2.148 GPa,

G_{xy} = 1.032 GPa,

Major Poisson ratio (v_{xy}) = 0.21,

Density = 1670 kg/m^3,

Properties of PVDF:

E = 63 GPa,

Poisson ratio = 0.31,

Density = 7500 kg/m^3,

Type of Laminate: Symmetric Laminate

Number of Laminas = 4;

Ply Thickness: 0.5 mm;

Pvdf Thickness: 0.1 mm;

Stacking sequence: [0_4]

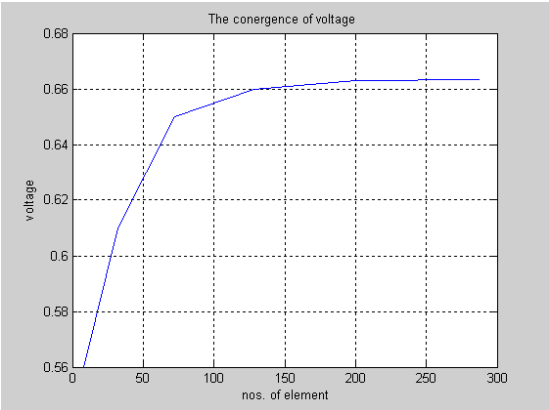

Figure2. Convergence of voltage output

4. Ribbon reinforced composite and damage detection:

Ribbon reinforced composite laminate are widely used in prosthetics–particularly in the field of orthodontics where canine-to-canine retention is carried out with the help of resin composite retainers reinforced with polyethylene/ Kevlar ribbons. There are certain advantages of using this type of composite in prosthetics:

1. Ribbon reinforced composites can have high strength and stiffness in two directions, longitudinal and in-plane direction. Thus such composites can be nearly isotropic in the plane of a sheet exhibiting nearly equal strength in all directions while the aligned-fiber composites, which have poor transverse strength.

2. They are less prone to crack and less care in handling.

3. They tend to very resistant to puncture by sharp objects.

4. Advantage of ribbon as reinforcement is that they can be packed in larger volume fractions than circular fibers.

The volume fraction of ribbons, V_r is given by

$$V_r = \frac{W_r t_r}{(W_r + W_m)(t_r + t_m)} = \frac{1}{[1+(W_m / W_r)][1+(t_m / t_r)]} \qquad (81)$$

Where W_r and t_r are respectively the width and thickness of the ribbons, t_m is the spacing between two layers of the ribbons, and W_m is the spacing between two ribbons in a layer

The longitudinal modulus of ribbon composites, like that of the continuous-fiber composites, is also given by the rule of the mixtures as

$$E_L = E_r V_r + E_m V_m \tag{82}$$

where E_r is the elastic modulus of ribbons. The in-plane transverse behavior of ribbon composites is analogous to the longitudinal behavior of aligned short-fiber composites. Therefore, the in-plane transverse modulus is given by the Halpin-Tsai equation as

$$\frac{E_T}{E_m} = \frac{1 + (2W_r / t_r)\eta_r V_r}{1 - \eta_r V} \tag{83}$$

Where

$$\eta_r = \frac{(E_r / E_m) - 1}{(E_r / E_m) + 2(W_r / t_r)}$$

These structures typically work like a bridge between the canines. They are subjected to central loading as well as support yielding due to unequal movement of the bridged canines. However, due to the high strain in the laminate, the chances of delamination and laminate failures are quite high in such microstructure.

Damage Detection:

There are mainly two types of damage in composite either there is ply failure or delamination failure. For considering ply failure we have neglected the stiffness contribution of that region to total stiffness of the system. For delamination a simple mechanics is followed. The constitutive equation for a laminated composite is

$$\begin{Bmatrix} N \\ M \end{Bmatrix} = \begin{bmatrix} A & B \\ B & D \end{bmatrix} \begin{Bmatrix} \varepsilon_0 \\ \kappa \end{Bmatrix} \tag{84}$$

For the upper part of the composite (i.e. above the delamination), the constitutive equation can be written as

$$\begin{Bmatrix} N_1 \\ M_1 \end{Bmatrix} = \begin{bmatrix} A_1 & B_1 \\ B_1 & D_1 \end{bmatrix} \begin{Bmatrix} \varepsilon_{01} \\ \kappa_1 \end{Bmatrix} \tag{85}$$

Where $\varepsilon_{01} = \varepsilon_0 + z_1\kappa$ and $\kappa_1 = \kappa$.

Similarly, for the lower part of composite (i.e. below the delamination), the constitutive equation is

$$\begin{Bmatrix} N_2 \\ M_2 \end{Bmatrix} = \begin{bmatrix} A_2 & B_2 \\ B_2 & D_2 \end{bmatrix} \begin{Bmatrix} \varepsilon_{02} \\ \kappa_2 \end{Bmatrix} \tag{86}$$

Where $\varepsilon_{02} = \varepsilon_0 + z_2\kappa$ and $\kappa_2 = \kappa$.

At the interface edge

$$N = N_1 + N_2 \tag{87}$$

$$M = M_1 + M_2 \tag{88}$$

Substituting equations (84 – 86) into equations (87-88), the new A, B and D matrix of delaminated composite is

$$\begin{bmatrix} A & B \\ B & D \end{bmatrix} = \begin{bmatrix} A_1 + A_2 & (A_1 z_1 + A_2 z_2) + (B_1 + B_2) \\ B_1 + B_2 & (B_1 z_1 + B_2 z_2) + (D_1 + D_2) \end{bmatrix} \tag{89}$$

So, stiffness matrix for delamination case will be asymmetric.

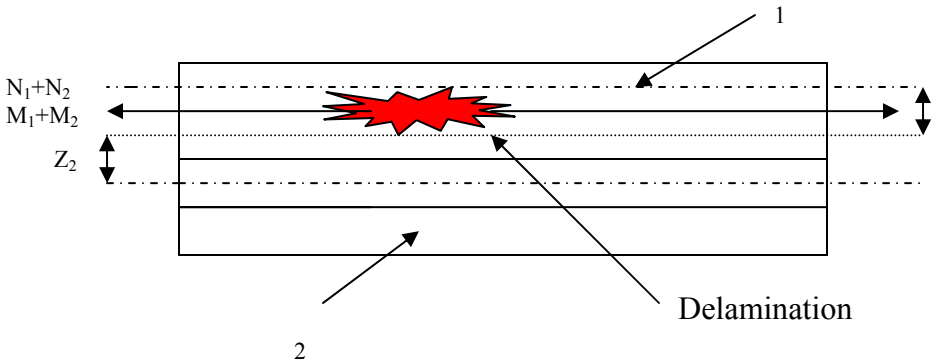

Figure3. Delamination phenomena in composite plate

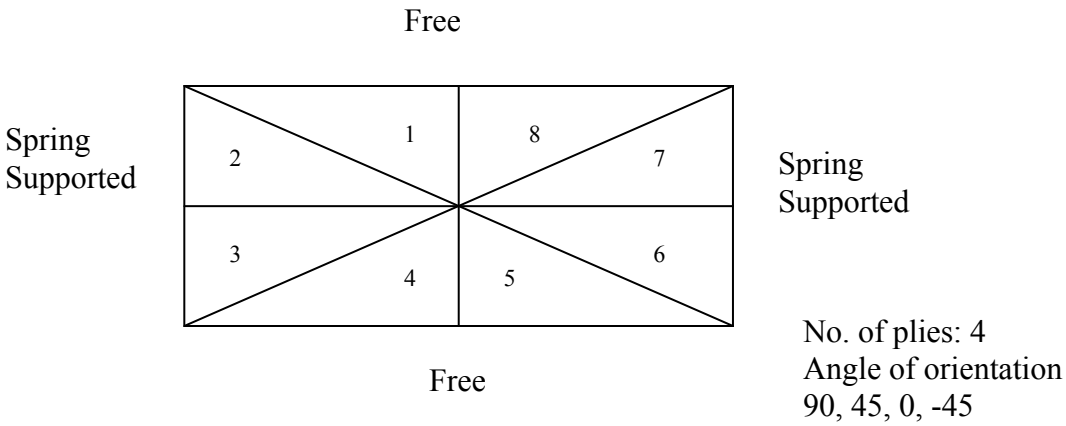

Figure4. Element Configuration (1)

Detail of Ribbon reinforced composite:

The length of plate: lx=25mm;

The width of plate: ly=1mm;

The thickness of plate: h= 1mm;

Fibre: Kevlar

Matrix: Polyethylene

The Elastic Properties:

Er=62GPa;

Em =0.889GPa;

Wr=200 μm;

B=20 μm;

Wm=10 μm;

tr=10 μm;

tm=10 μm ;

Spring Constant =100N/m;

Force given F(t) = 10(1+cos(wt))N

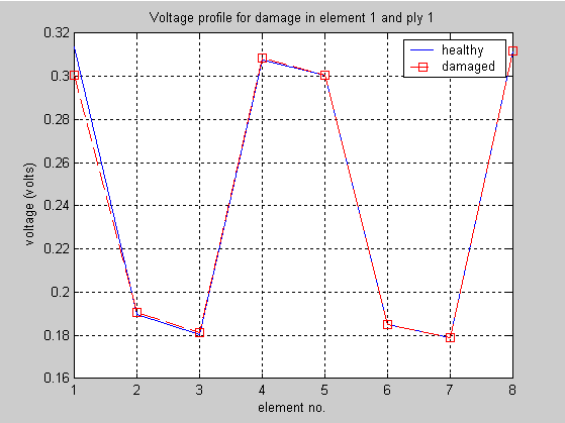

Figure5. Voltage Profile for damage in element 1 and ply1 for configuration (1)

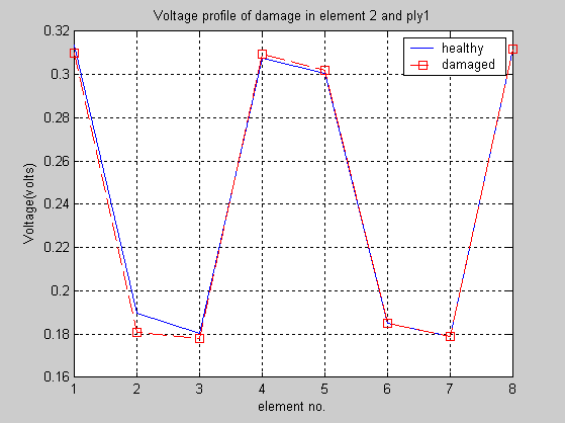

Figure6. Voltage Profile for damage in element 2 and ply1 for configuration (1)

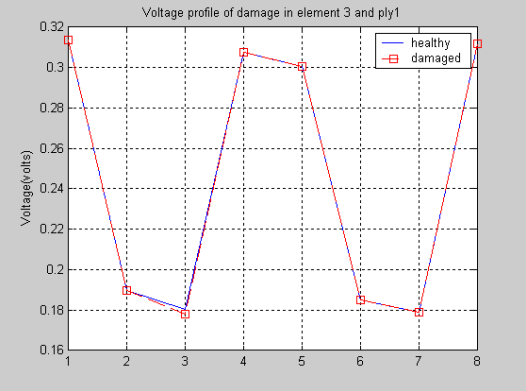

Figure7. Voltage Profile for damage in element 3 and ply1 for configuration (1)

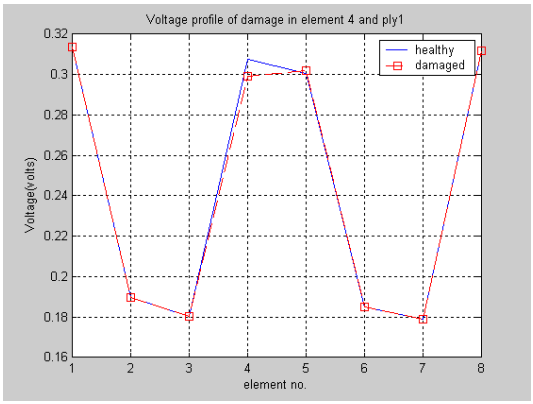

Figure8. Voltage Profile for damage in element 4 and ply1 for configuration (1)

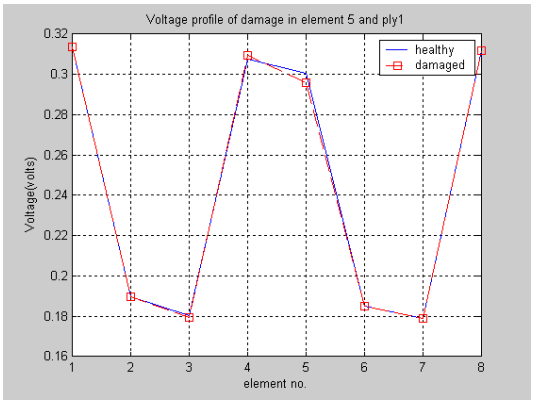

Figure9. Voltage Profile for damage in element 5 and ply1 for configuration (1)

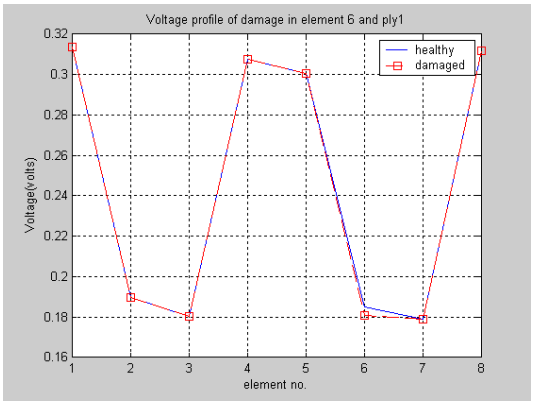

Figure10. Voltage Profile for damage in element 6 and ply1 for configuration (1)

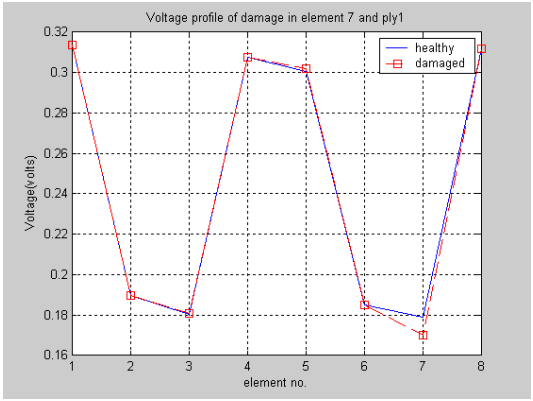

Figure11. Voltage Profile for damage in element 7 and ply1 for configuration (1)

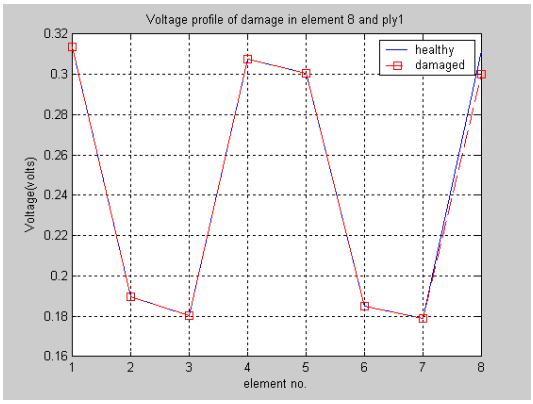

Figure12. Voltage Profile for damage in element 8 and ply1 for configuration (1)

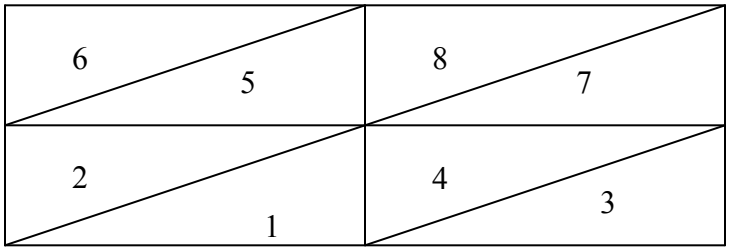

Figure13. Element Configuration (2)

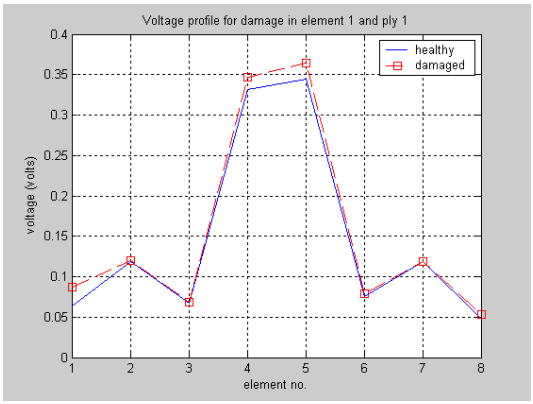

Figure14 Voltage Profile for damage in element 1and ply1 for configuration (2)

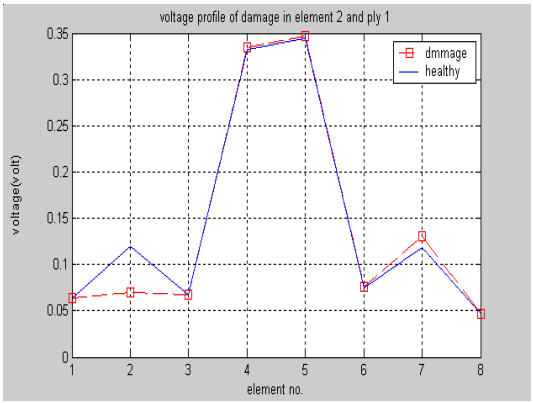

Figure15. Voltage Profile for damage in element 2 and ply1 for configuration (2)

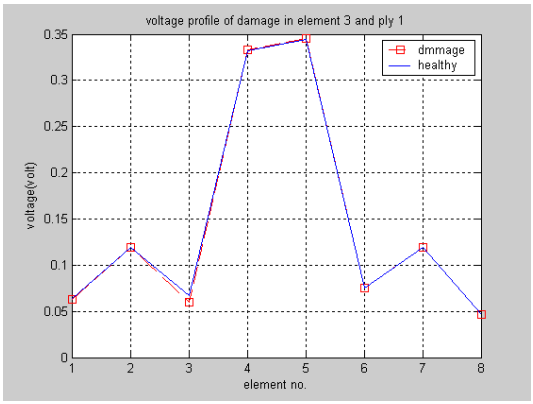

Figure16. Voltage Profile for damage in element 3 and ply1 for configuration (2)

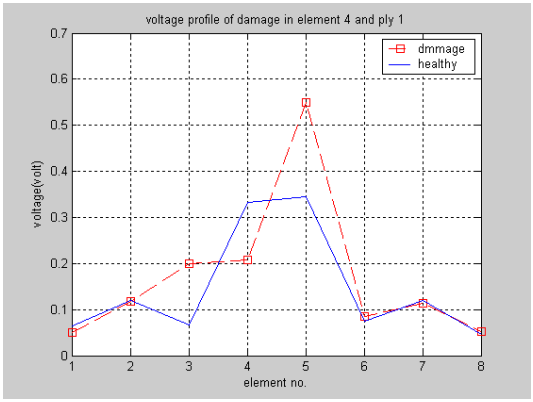

Figure17. Voltage Profile for damage in element 4 and ply1 for configuration (2)

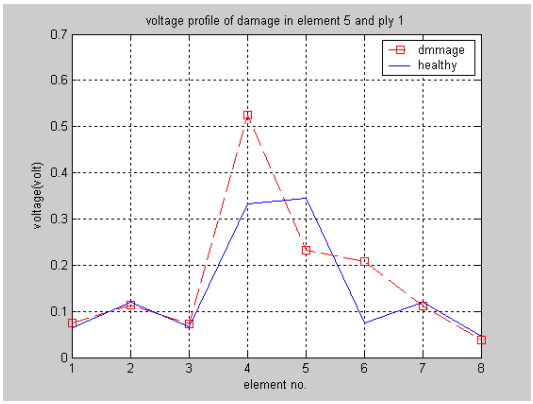

Figure18. Voltage Profile for damage in element 5 and ply1 for configuration (2)

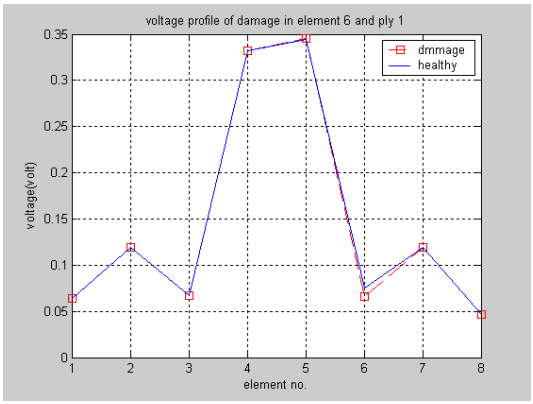

Figure19. Voltage Profile for damage in element 6 and ply1 for configuration (2)

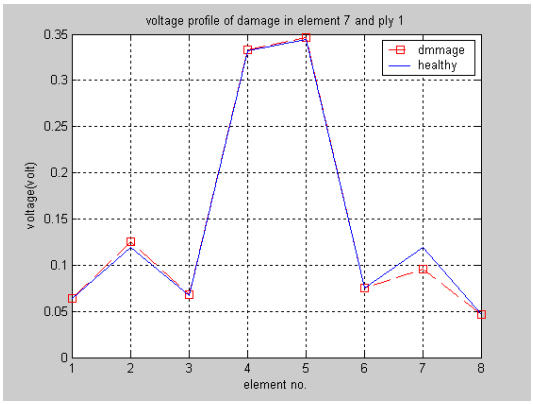

Figure20. Voltage Profile for damage in element 7 and ply1 for configuration (2)

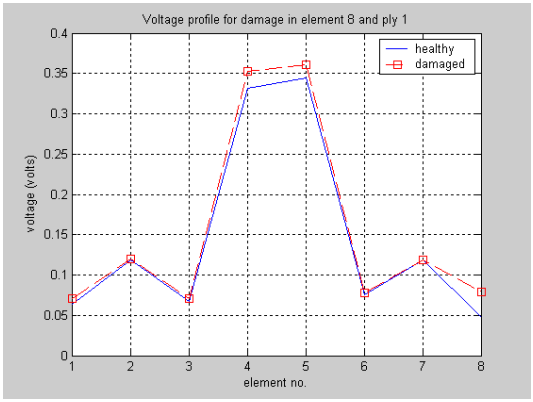

Figure21. Voltage Profile for damage in element 8 and ply1 for configuration (2)

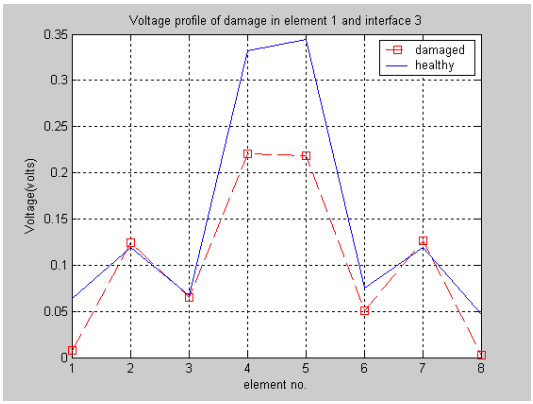

Figure22. Voltage Profile for damage in element 1 and interface3 for (2)

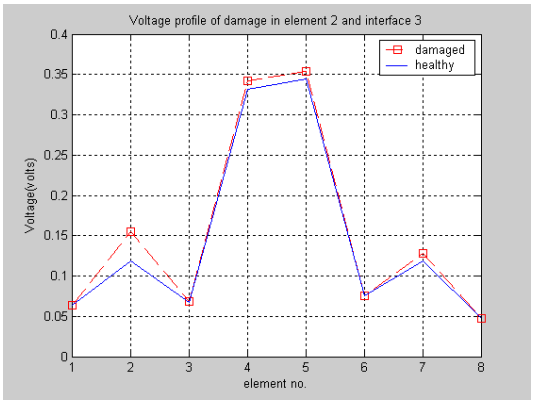

Figure23. Voltage Profile for damage in element 2 and interface 3 for (2)

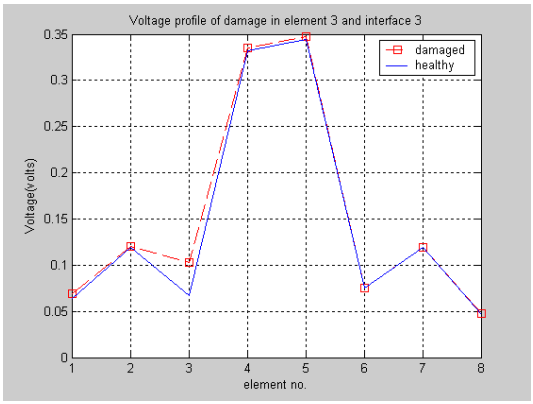

Figure24. Voltage Profile for damage in element 3 and interface 3 for (2)

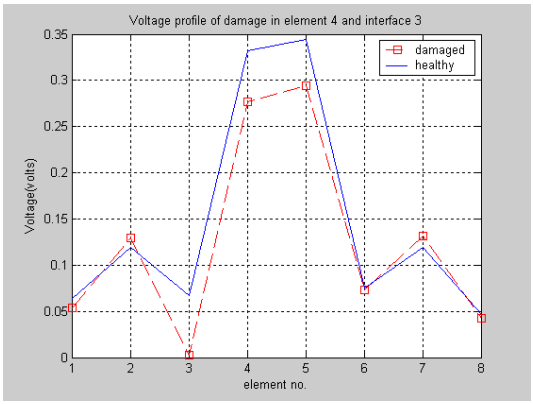

Figure25. Voltage Profile for damage in element 4 and interface3 for (2)

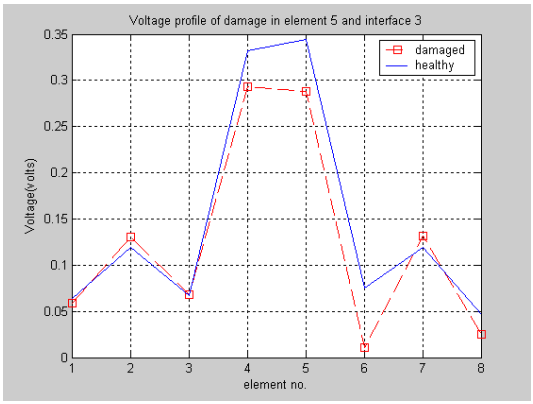

Figure26. Voltage Profile for damage in element 5 and interface3 for (2)

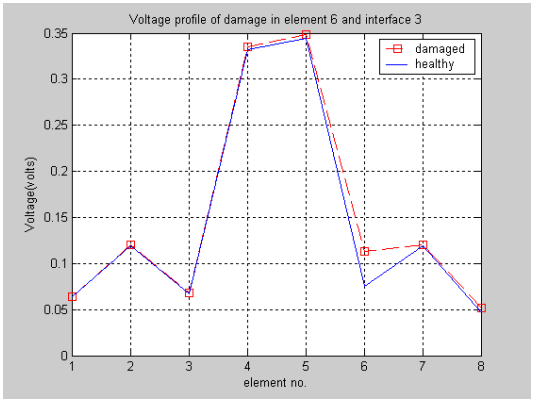

Figure27. Voltage Profile for damage in element 6 and interface 3 for (2)

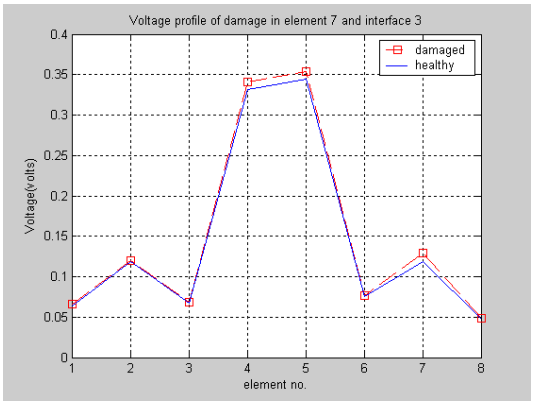

Figure28. Voltage Profile for damage in element 7 and interface3for (2)

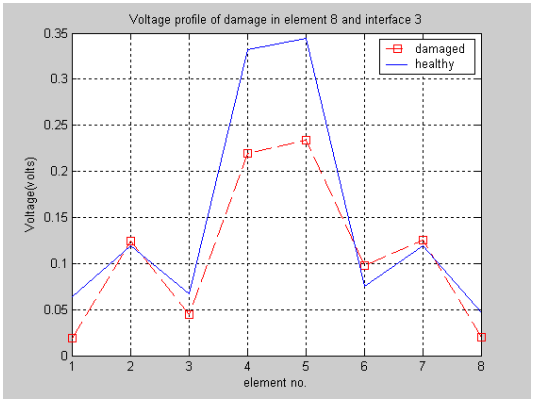

Figure29. Voltage Profile for damage in element 8 and interface3for (2)

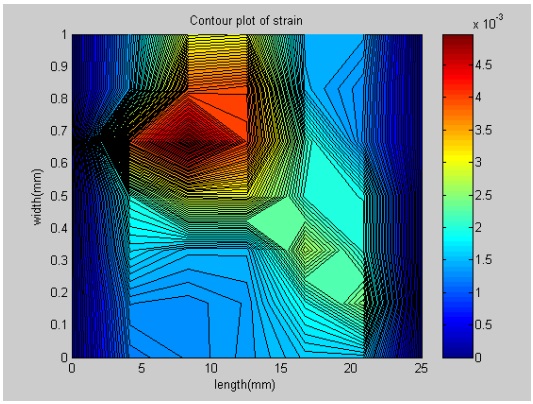

Figure30. Strain profile for damage in element 4, ply 1 and configuration (2)

Since for the element configuration 1 the problem of mechanical impedance can be analysed for the quarter portion i.e. element 1 and 2

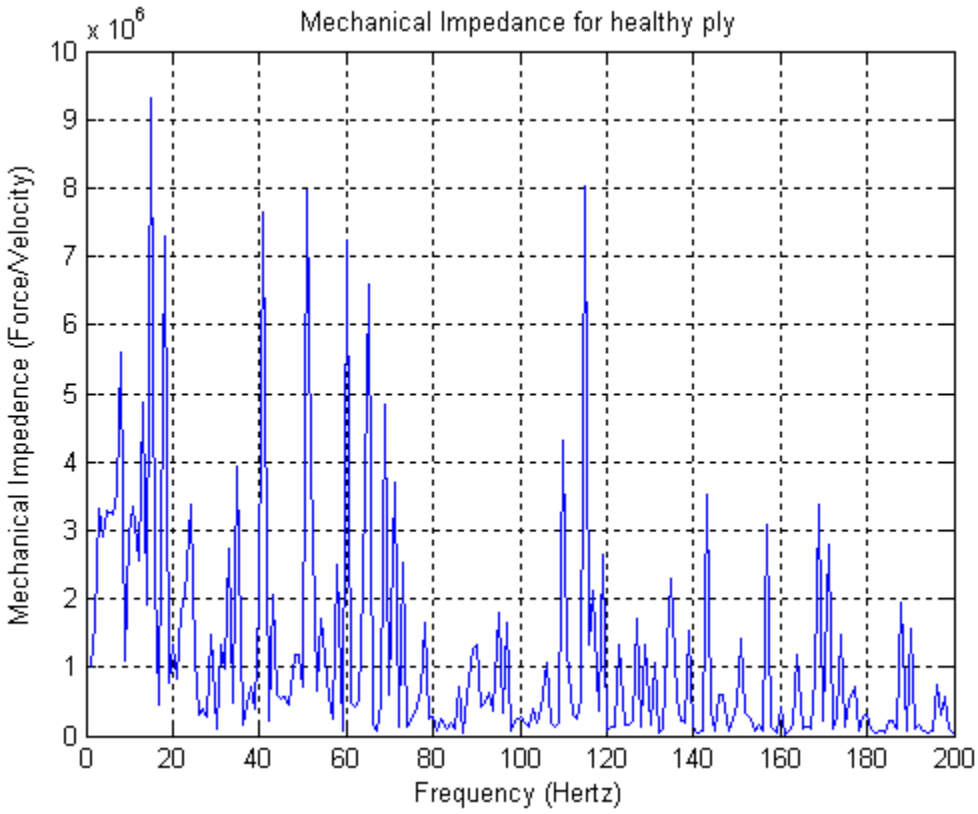

Figure31. Mechanical Impedance for healthy ply for configuration1

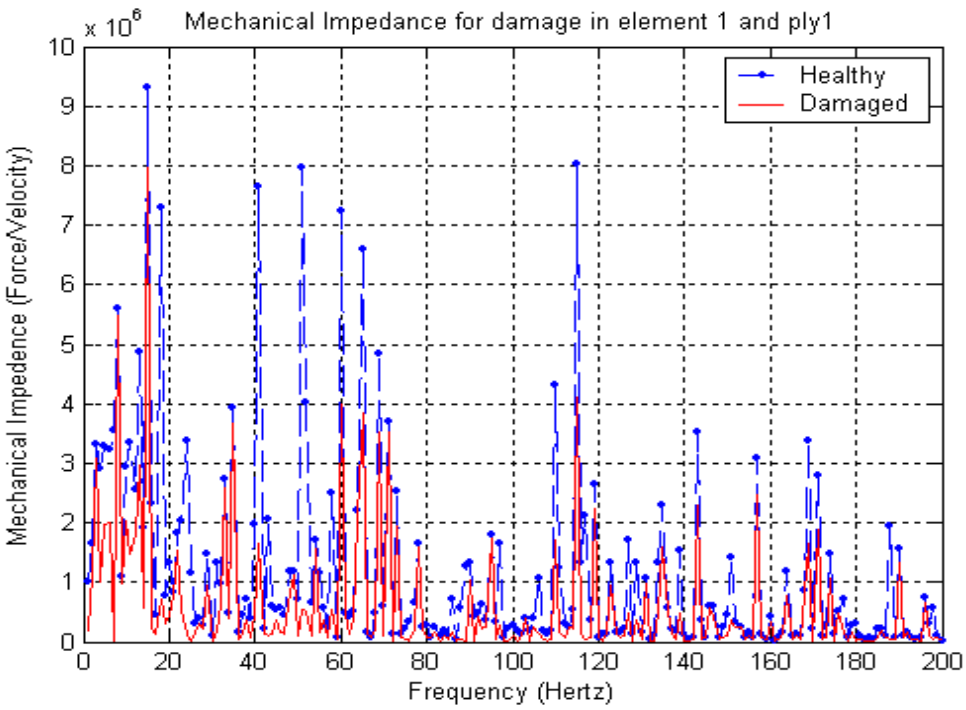

Figure32. Mechanical Impedance for damage in element 1 and ply1 for configuration1

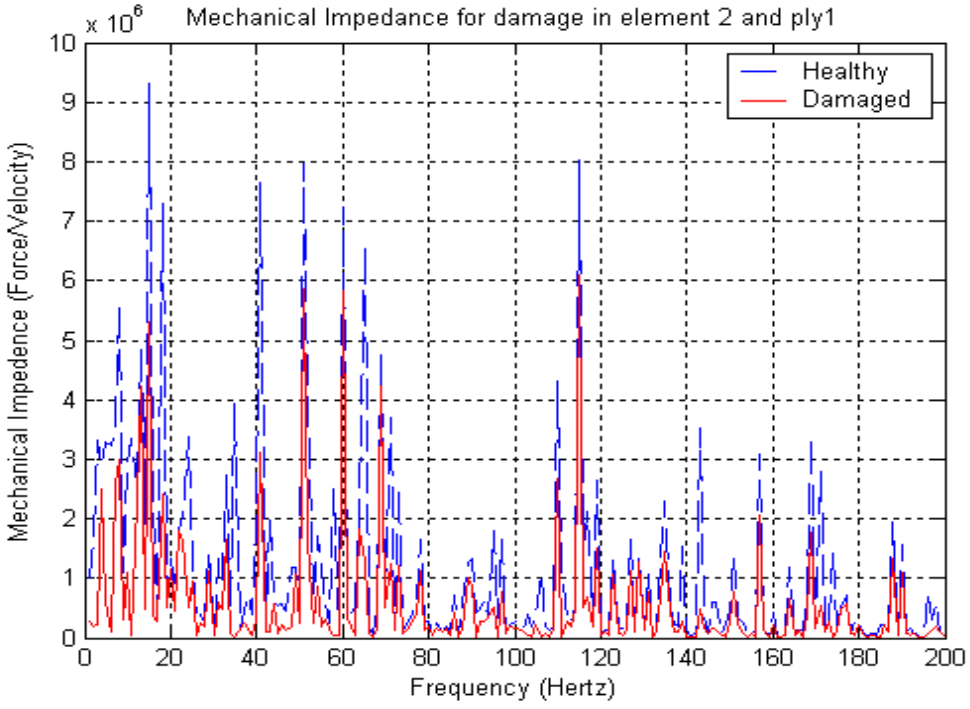

Figure33. Mechanical Impedance for damage in element 2 and ply1 for configuration1

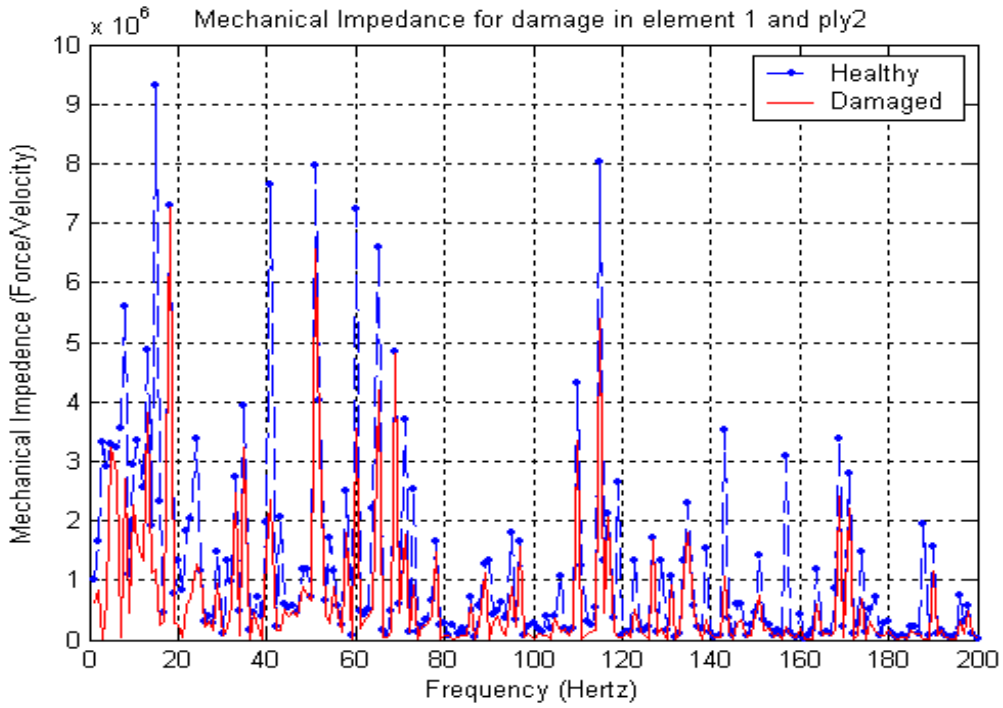

Figure34. Mechanical Impedance for damage in element 1 and ply2 for configuration1

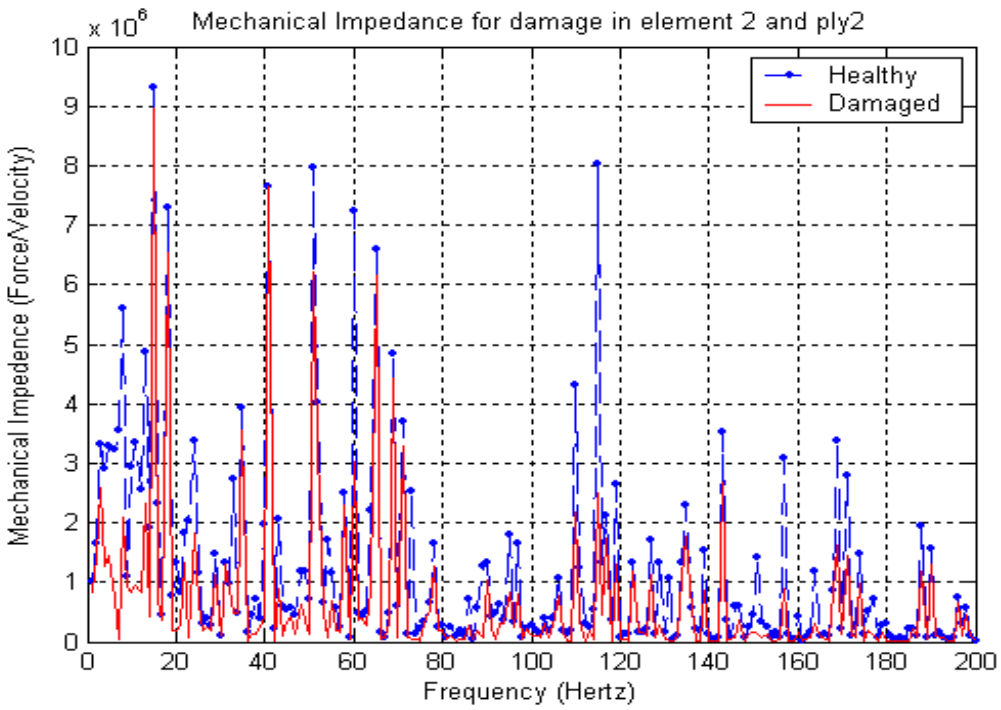

Figure35. Mechanical Impedance for damage in element 2 and ply2 for configuration1

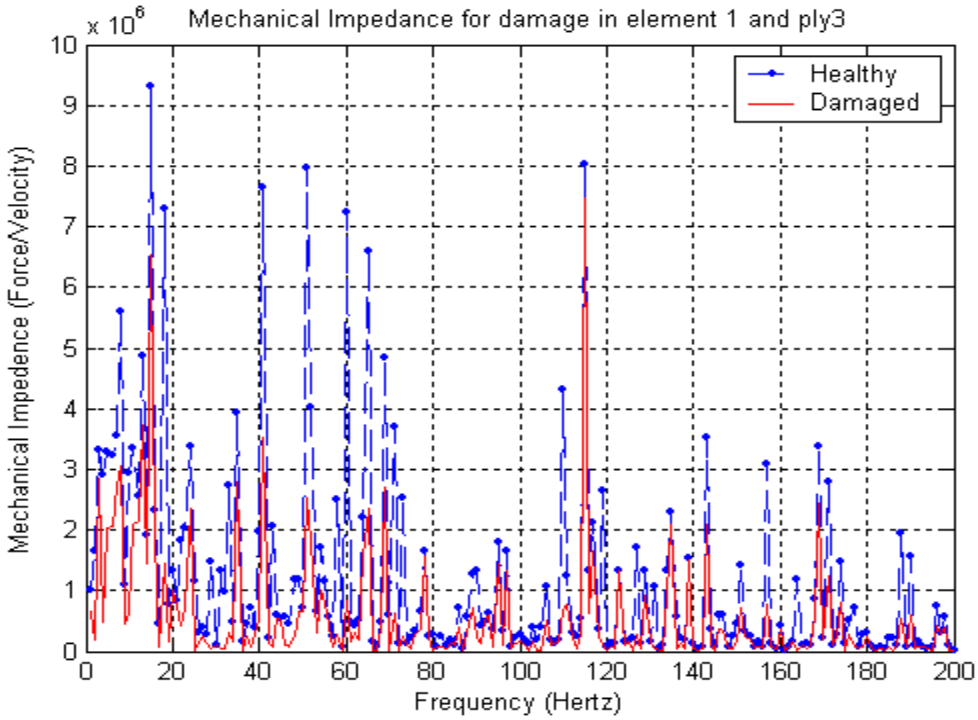

Figure36. Mechanical Impedance for damage in element 1 and ply3 for configuration1

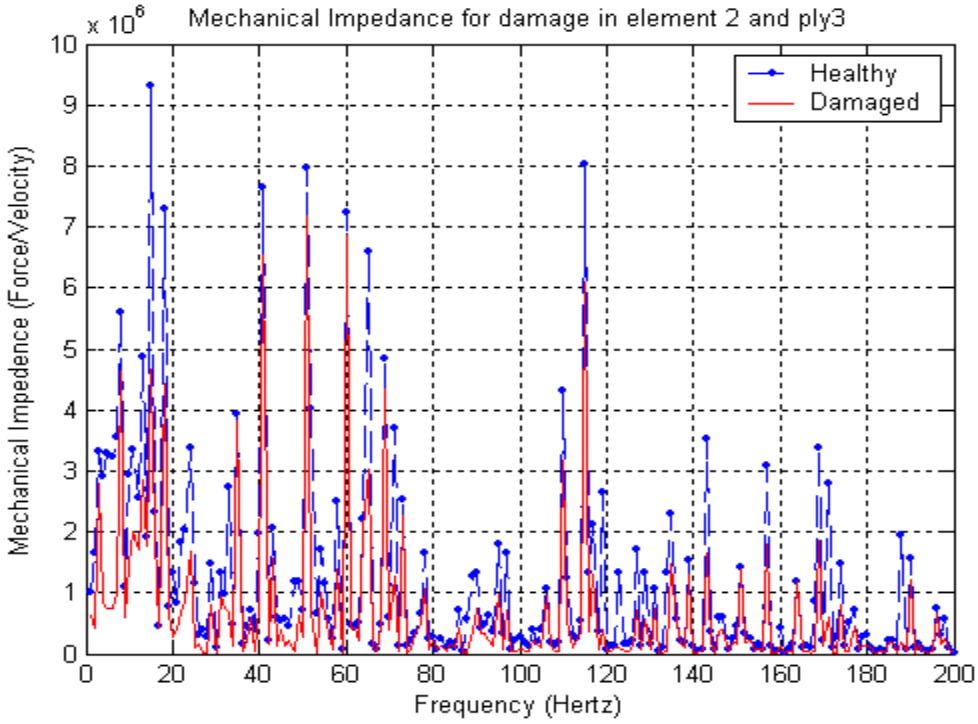

Figure37. Mechanical Impedance for damage in element 2 and ply3 for configuration1

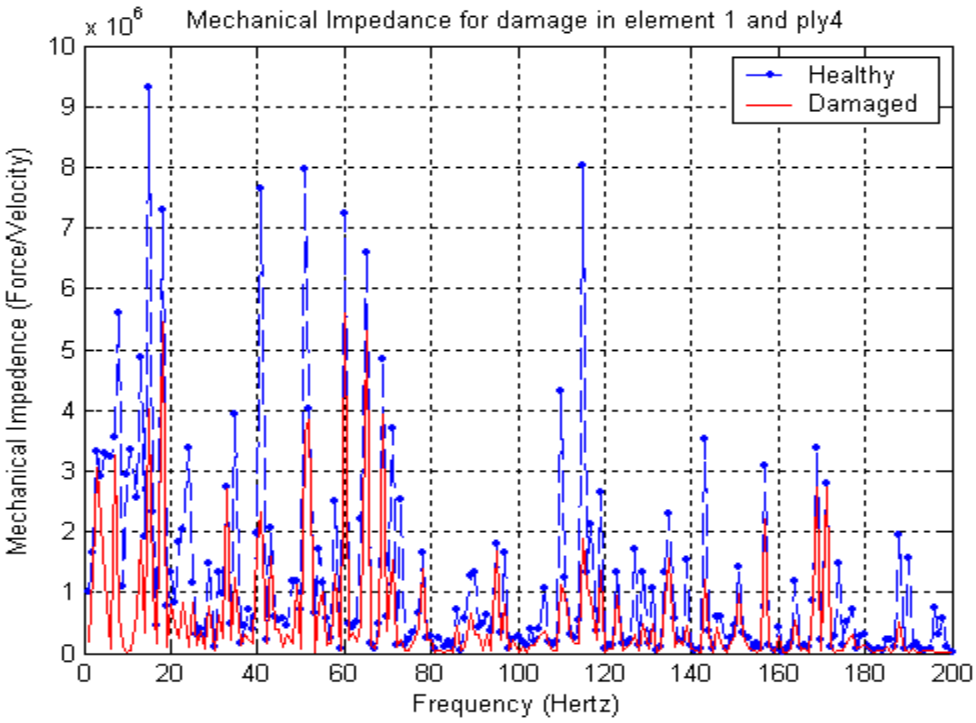

Figure38. Mechanical Impedance for damage in element 1 and ply4 for configuration1

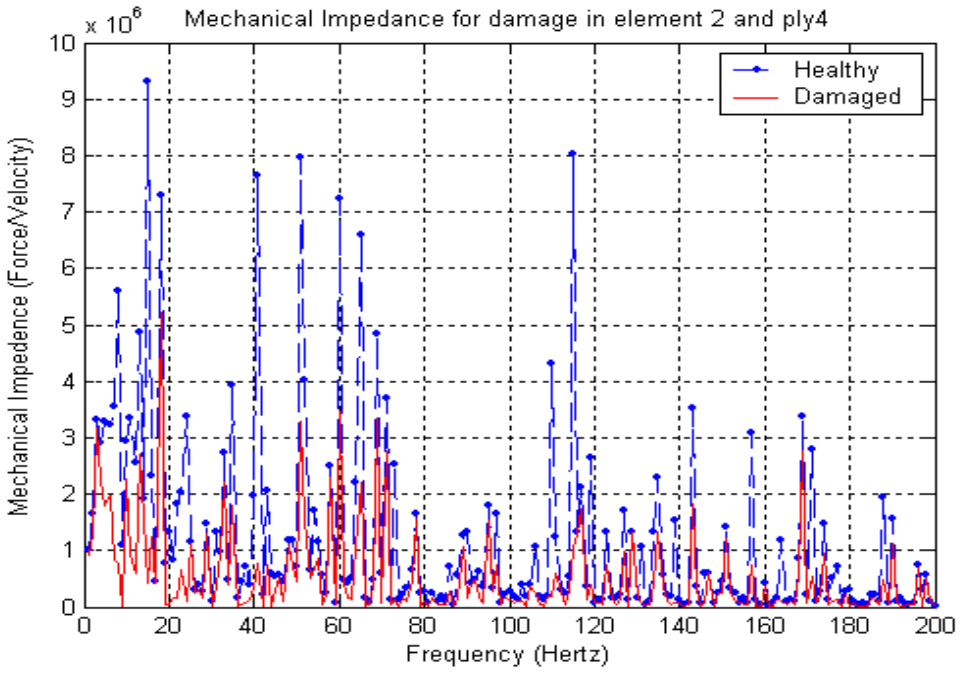

Figure39. Mechanical Impedance for damage in element 2 and ply4 for configuration1

5. Conclusion:

The voltage profile is compared both for healthy and damaged composite. The element configuration 1 is symmetric and in results we can see that the voltage decreases at the point of damage. The element configuration 2 is symmetric about it diagonal so results symmetry according to it. The voltage profile for damage in element 4 and 5 shows some different result compare to other elements. One reason is that we are using only eight elements due to difficulty in attaching pvdf sensor and taking lots of result. The strain profile for damage in element 4 and configuration 2 is shown in figuire30 to convince the reader.

Voltage profile for delamination is showing unsymmetric behavior because the stiffness matrix is not symmetric. Figure 31 shows the mechanical impedance for healthy ply. In figures (31-39) it is compared with damaged composite. Here these results show a decrement in mechanical impedance when there is damage. Sine the stiffness of a body decreases when there is a damage, the velocity is going to increase and mechanical impedance is a ratio of force by velocity so it shows a decrement behaviour.

So, knowledge based database is created for ribbon reinforced composite for both ply failure and delamination. The results of dynamic analysis are expected to help in efficient damage diagnosis for these kinds of structures.

6. Reference:

[1] D D L Chung 2001 Structural health monitoring by electrical resistance measurement *Smart Material and Structure* **10** 624-636

[2] Panedy, A. K.Biswas amd Samman M 1991 Damage detection from changes in curvature mode shapes *Journal of Sound and Vibration* 145, **2** 321-332

[3] Tierang Liu, Martin Veidt and Sritawat Kitipornchal 2003 modelling the input-output behaviour of piezoelectric structural health monitoring systems for composite plates *Smart Material & Structure* **12** 836-844

[4] Staszewski P 2003 Quick inspection of large structures using low frequency ultrasound Structural Health Monitoring: CurrentStatus and Perspectives ed F-K Chang (Lancaster: Technomic Publishing): 529–40

[7] G. R. Cowper, E. Kosko, G. M. Lindberg, and M. D. Olson 1969 Static and Dynamic applications of a high-precision triangular plate bending element. *AIAA Journal*, 7(10): 1957-1965

[8] G. R. Cowper, G. M. Lindberg and M. D. Olson 1970A shallow shell finite element of triangular shape. *Int. Journal of Solids Structures* 6: 1133-1156

[9] C. Jeyanchandrabose and J. Kirkhope 1985 Explicit Formulation for a high precision triangular laminated anisotropic laminated anisotropic thin plate finite element. *Computers & Structures*, 20(6): 991-1007

[10] B. Bhattacharya. 1998 PhD. Thesis